

# Systematic TLM Measurements of NiSi and PtSi Specific Contact Resistance to n- and p-Type Si in a Broad Doping Range

N. Stavitski, *Student Member, IEEE*, M. J. H. van Dal, A. Lauwers, C. Vrancken, A. Y. Kovalgin, and R. A. M. Wolters

**Abstract**—We present the data on specific silicide-to-silicon contact resistance ( $\rho_c$ ) obtained using optimized transmission-line model structures, processed for a broad range of various n- and p-type Si doping levels, with NiSi and PtSi as the silicides. These structures, despite being attractive candidates for embedding in the CMOS processes, have not been used for NiSi, which is the material of choice in modern technologies. In addition, no database for NiSi–silicon contact resistance exists, particularly for a broad range of doping levels. This letter provides such a database, using PtSi extensively studied earlier as a reference.

**Index Terms**—NiSi, PtSi, silicide, specific contact resistance, transmission-line model (TLM).

## I. INTRODUCTION

**M**ETAL SILICIDES are being widely used in semiconductor manufacturing for years [1]. These silicides show metallic conductivity [1]. The metal silicide is formed as a result of heat treatment of a metal–semiconductor contact. The silicide–silicon junction is expected to behave similar to a metal–semiconductor contact, providing low line and contact resistance. Furthermore, for commonly used silicides, the silicide–silicon interface is free of contaminations due to the formation mechanism [2]. Contacts formed in this manner generally show stable electrical characteristics and exhibit very good mechanical adhesion [2]. Silicide–silicon contacts are therefore of considerable importance in silicon technology for providing contacts to source, drain, and gate of a MOSFET. Ultrashort channel MOSFETs with self-aligned silicide contacts are required for high-speed circuits. Thus, the ability to accurately measure the contact resistance of silicon-to-silicide junctions is essential for the development of the contact process.

Manuscript received December 14, 2007; revised January 17, 2008. This work was supported by NXP Research Leuven. The review of this letter was arranged by Editor M. Ostling.

N. Stavitski and A. Y. Kovalgin are with the MESA+ Institute for Nanotechnology, Chair of Semiconductor Components, University of Twente, 7500 AE Enschede, The Netherlands (e-mail: n.stavitski@utwente.nl).

M. J. H. van Dal is with NXP Research Leuven, 3001 Leuven, Belgium.

A. Lauwers and C. Vrancken are with IMEC, 3001 Leuven, Belgium.

R. A. M. Wolters is with the MESA+ Institute for Nanotechnology, Chair of Semiconductor Components, University of Twente, 7500 AE Enschede, The Netherlands, and also with the NXP Research Eindhoven, 5656 AA Eindhoven, The Netherlands.

Digital Object Identifier 10.1109/LED.2008.917934

## II. MOTIVATION

The contact resistance of silicide–semiconductor junctions has been extensively studied using various methods and structures, although the results show considerable scatter [3]. Moreover, some values for NiSi can be found in the literature [4]–[7], but no solid database for NiSi–silicon contact resistance exists, particularly for a broad range of doping levels. Most of the research studying  $\rho_c$  used cross-bridge Kelvin resistor (CBKR) structures, while in modern IC technology, one would tend to use transmission-line model (TLM) structures as they could be easier embedded in the standard self-aligned silicide CMOS process [8]. The advantage of the TLM structure over the CBKR one is that, in TLM structures, the silicide segments and the contact pads are made in one single-silicide process step. This allows one to define critical dimensions and makes in-line process control possible. The known accuracy problem of CBKR structures, while extracting low specific-contact-resistance values, was the other reason for us to choose the optimized TLM structures instead of CBKR structures. Furthermore, the extraction of the specific contact resistance, determined either by CBKR or TLM structures, resulted in different values (orders of magnitude difference) for a given doping level [3]. Our purpose is to compare the results obtained from our optimized, in terms of the silicide lengths and the number of segments, TLM structures with the data known from literature for PtSi and provide systematic measurement data for NiSi.

## III. EXPERIMENTAL APPROACH

The behavior of silicide–silicon junctions is similar to that of metal–semiconductor junctions. Therefore, the contact resistance, defined as the reciprocal derivative of current density with respect to the voltage [9], is determined mainly by the thermionic-emission-current transport mechanism for contacts with lower doping concentrations [9]. For contacts with higher doping levels, the tunneling process dominates. Hence, the specific contact resistance depends strongly on doping concentration and varies exponentially with  $(\phi_{Bn}/\sqrt{ND})$  [9]. To verify the consistency of the extracted contact resistance, it was decided to evaluate a wide range of doping levels ( $10^{18}$ – $10^{21}$  cm<sup>-3</sup>) of p- and n- type Si contacts to NiSi and PtSi. Deep junctions were chosen in order to enable an accurate measurement of the doping profiles and, therefore,

to minimize errors during the extraction of the specific contact resistance. Moreover, for deeper junctions, the relative (to the junction depth) silicon consumption is lower. This also increases the validity of our measurements, resulting in a smaller relative change of the doping profile (and, therefore, the sheet resistance), which can be expected when silicon is consumed, since the sheet resistance of the semiconductor immediately beneath the contact is an important part of the contact resistance/resistivity. NiSi and PtSi silicides are chosen because of their technological importance. NiSi is widely used in advanced CMOS [10]. It has a resistivity comparable to that of commonly used  $\text{TiSi}_2$  and  $\text{CoSi}_2$ . NiSi can be formed at low temperatures, and less silicon is consumed [11]–[13]. In addition, NiSi has no agglomeration problems on narrow lines [14]–[16]. On the other hand, PtSi has been studied thoroughly [3], [17]–[19], providing a good reference. Silicide-to-silicon contact resistance was investigated using a set of optimized test structures with silicided segments of varying lengths, based on the Scott model for TLM structures [8], [20]. The validity of our results is based on the following: 1) systematic measurements and statistical data analysis (i.e., the represented data were averaged over 18 dies for each doping type and concentration), 2) experimental verification of the actual active doping concentrations and doping profiles by secondary ion-mass spectrometry (SIMS) and spreading-resistance-probe (SRP) techniques, 3) verification of the actual silicide lengths for different silicide segments by TEM analysis, and 4) optimizing the TLM structures in terms of the silicide lengths and the number of segments. The latter was a result of analyzing the existing TLM-structure design features that we use and by other researchers in their previous work [8], [20]. The optimized structures provided a better fit and a higher accuracy using the Scott method and, therefore, supported the data verification.

#### IV. RESULTS

The (100) p-type Si wafers were used as starting material for the contact-resistance study. The active areas were defined by Shallow Trench Isolation, and the channels were defined by I-line lithography. Doping concentrations were achieved by low-dose well implantations of B (180 keV) or P (420 keV) for the p-well or n-well, respectively. As and B implantations, followed by spike annealing, were carried out for n- and p-highly doped drain (HDD) areas, respectively. The doses and energies were adjusted to cover the  $10^{21}$ – $10^{18}$   $\text{cm}^{-3}$  doping-concentration range. In order to verify the actual concentrations, the same implantation recipes were applied to blanket wafers, and the total doping concentration and the concentration of electrically active impurities were determined by SIMS and SRP techniques respectively. The results agreed very well with the given energies and doses used. The concentration profiles are shown in Fig. 1.

For the TLM structures, a silicide blocking layer ( $\text{SiO}_2/\text{Si}_3\text{N}_4$ ) was deposited and patterned using deep ultraviolet lithography. The silicided segments were made on the n- and p-HDD areas with two different silicide widths ( $W$ ) of 2 and  $8 \mu\text{m}$  and silicide lengths ( $L$ ) ranging from 0.1 to  $3 \mu\text{m}$ , chosen

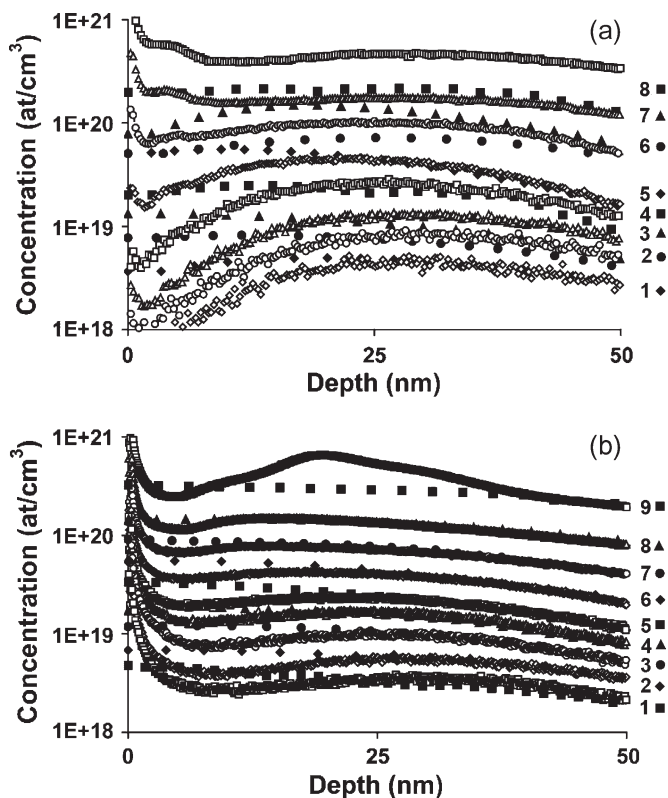


Fig. 1. (a) As and (b) B concentration profiles of (a) n- and (b) p-HDD areas obtained by (open symbols) SIMS and (solid symbols) SRP. Each symbol type corresponds to a given profile. Active doping concentrations ( $\times 10^{19}$ , per cubic centimeter) at 20 nm used for  $\rho_c$  extraction: for (a): 0.5 (1), 0.79 (2), 1.2 (3), 2.1 (4), 4.7 (5), 7.1 (6), 15 (7), 19 (8); for (b): 0.31 (1), 0.61 (2), 1.0 (3), 1.7 (4), 2.5 (5), 4.6 (6), 8.3 (7), 14 (8), 30 (9).

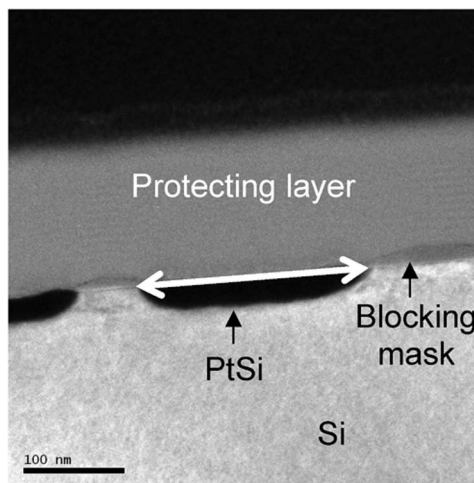


Fig. 2. TEM cross section of PtSi on p-HDD for  $n = 100$ . The arrow depicts the location where the length was measured.  $\text{Si}_3\text{N}_4/\text{Pt}$  is used as a protecting layer for TEM sample preparation.

to cover the entire range  $L$  values in the Scott fit. Thus, each TLM structure consisted of a number of fragments, where each fragment comprised  $n$  silicided segments of length  $L$ . The number of segments  $n$  varied from 0 to 150. Finally, a 10-nm-thick Ni layer or a 13-nm-thick Pt layer was deposited, and the silicide was formed by either two-step annealing ( $300^\circ\text{C}$  for 43 s +  $470^\circ\text{C}$  for 43 s) for NiSi or one-step annealing ( $500^\circ\text{C}$

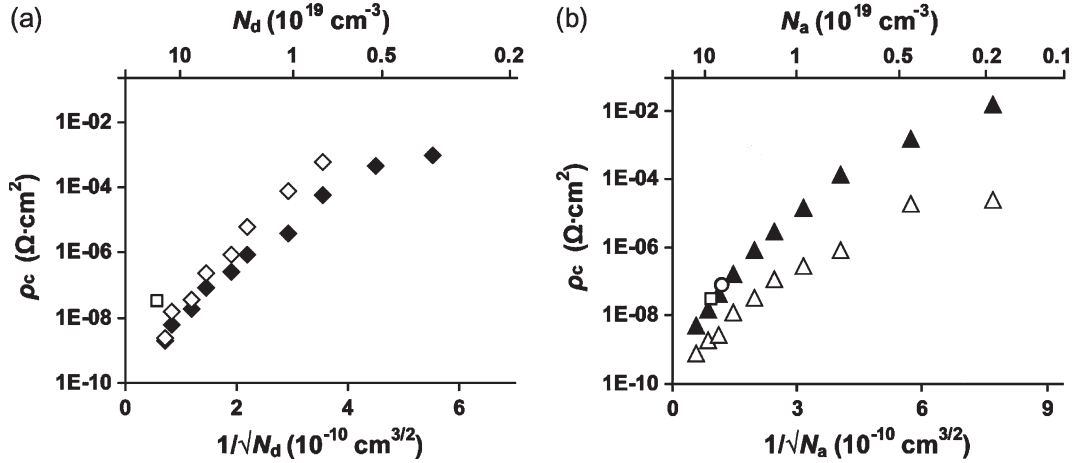


Fig. 3. (a) Specific contact resistances to n-HDD as a function of the doping level: NiSi from this letter ( $\blacklozenge$ ), PtSi from this letter ( $\diamond$ ), and PtSi from [17] ( $\square$ ). (b) Specific contact resistances to p-HDD as a function of the doping level: NiSi from this letter ( $\blacktriangle$ ), PtSi from this letter ( $\triangle$ ), PtSi from [17] ( $\square$ ), and PtSi from [18] ( $\circ$ ).

for 30 s) for PtSi. In both cases, the unreacted metal was selectively removed by wet etching.

The silicide profiles and lengths for NiSi and PtSi were verified by TEM analysis using a FEI Tecnai F30ST TEM operated at 300 kV (see Fig. 2).

Resistance values  $R_{\text{ref}}$  and  $R_i$  of all the fragments were measured, as explained in [20]. The fitting of the obtained  $R_{\text{cmeas}}$  values with the Scott model [20] was carried out to extract the specific contact resistances. The specific contact resistances, plotted as a function of the doping levels ( $1/\sqrt{N}$ ) for n- and p-HDD, are shown in Fig. 3. The doping levels were taken from the SRP profiles at 20-nm depth, as they represented the relevant electrically active concentrations of HDD areas after the 20-nm-thick silicide had been formed.

## V. DISCUSSION AND CONCLUSION

Except for the highest concentrations ( $10^{21} \text{ cm}^{-3}$  for B and  $10^{20}$ – $10^{21} \text{ cm}^{-3}$  for As), all the dopants were activated showing good match between the results obtained by SIMS and SRP methods (Fig. 1). The first 10 nm of the SIMS curves cannot be compared with the results obtained by SRP because of the known SIMS accuracy problem for the upper layer. However, this fact does not compromise the interpretation of the results, since the relevant active concentrations are at 20–30-nm depth, as the upper silicon layer is consumed during the silicide formation.

It was found that  $\rho_c$  decreased with increasing As or B concentration, as expected from theory [9]. For lower As concentrations, PtSi to n-type silicon contact resistance was slightly higher than that of NiSi to n-type silicon [Fig. 3(a)]. It is known that, at high doping levels, the effective barrier height for the given metal–semiconductor contacts can be lower [9]. The similar values of specific contact resistance to silicon for PtSi and NiSi at high doping levels, shown in Fig. 3, are due to a convergence of the effective barrier height for these silicides. PtSi contacts to p-type silicon exhibited the lowest contact resistance at lower doping in agreement with the lower Schottky barrier [2]. A detailed discussion of the experimental

results in light of transport mechanisms will be included in our future publications.

PtSi to n-type silicon  $\rho_c$  values, known from literature, range from  $3$ – $4 \cdot 10^{-4}$  to  $4 \cdot 10^{-8} \Omega \cdot \text{cm}^2$  for doping concentrations between  $5 \cdot 10^{18}$  and  $3 \cdot 10^{20} \text{ cm}^{-3}$  [3]. For low concentrations ( $3 \cdot 10^{19} \text{ cm}^{-3}$  and below), our results are in agreement with the results previously obtained using other methods. For concentrations of  $10^{20} \text{ cm}^{-3}$  and higher, a disagreement appears. For example, Cohen *et al.* [17] determined a  $\rho_c$  of  $3.7$ – $5 \cdot 10^{-8} \Omega \cdot \text{cm}^2$  at an As concentration of  $3 \cdot 10^{20} \text{ cm}^{-3}$ , whereas, in this letter, a value of  $1.5 \cdot 10^{-8} \Omega \cdot \text{cm}^2$  is found at an As concentration of  $1.9 \cdot 10^{20} \text{ cm}^{-3}$  [Fig. 3(a)]. The difference can be explained by the fact that most of the measurements presented in the literature have been performed using SIMS analysis for determining the dopant concentration. The active concentrations for the highest doses might be lower, as shown in this letter. This could crucially affect the contact-resistance value. From our results for PtSi to n-type silicon, a change of two orders of magnitude in the doping range of  $1.9 \cdot 10^{20}$  to  $4.7 \cdot 10^{19} \text{ cm}^{-3}$  was seen.

The  $\rho_c$  results of PtSi to p-type silicon is a similar case. For a low concentration of  $\sim 10^{18} \text{ cm}^{-3}$ , our results fall in the expected range [3]. For higher concentrations, in particular  $10^{19} \text{ cm}^{-3}$  and above, the difference becomes larger. Reported values are  $4 \cdot 10^{-8}$  and  $7.4 \cdot 10^{-8} \Omega \cdot \text{cm}^2$  for B concentrations of  $1.2 \cdot 10^{20}$  and  $7 \cdot 10^{19} \text{ cm}^{-3}$ , respectively [17], [18]. In this letter, much lower  $\rho_c$  values of  $1.9 \cdot 10^{-9}$  and  $2.8 \cdot 10^{-9} \Omega \cdot \text{cm}^2$  have been determined for a similar B concentration, i.e.,  $1.4 \cdot 10^{20}$  and  $8.2 \cdot 10^{19} \text{ cm}^{-3}$  [Fig. 3(b)]. In addition to the fact that the exact concentrations of the active As/B were not always verified, a possible explanation of the difference is the known accuracy problems during the data extraction using CBKR structures in the range of  $\sim 10^{-8} \Omega \cdot \text{cm}^2$  and below [21]. In this case, the current-crowding effect may lead to significant errors (orders of magnitude) [3], [22]. Yet, another factor that complicates the data comparison is that, in some cases, different processing and measurement techniques were used.

Using systematic measurements of optimized TLM structures to determine PtSi-to-silicon  $\rho_c$ , the differences with the

literature values have been explained in terms of active doping concentrations and CBKR measurements limitations. Based on our PtSi-to-silicon  $\rho_c$  study, the  $\rho_c$  values obtained for NiSi-to-silicon were validated. The NiSi data were obtained from structures fabricated in a CMOS technology, using standard salicide recipe. These very low values further favor the use of NiSi in modern CMOS processes in terms of the similar values obtained on both n- and p-type silicon. Finally, we created a unique database for NiSi-to-silicon  $\rho_c$  for a wide range of doping levels, which is important for the development of the modern contact technology.

#### ACKNOWLEDGMENT

The authors would like to thank the IMEC P-line for processing the wafers. They would also like to thank IMEC and Philips Research Materials Analysis Groups for SRP and SIMS measurements. They would also like to thank M. Kaiser for the TEM work.

#### REFERENCES

- [1] S. Wolf and R. N. Tauber, *Silicon Processing for the VLSI Era*, vol. 2. Sunset Beach, CA: Lattice Press, 1986.
- [2] E. H. Rhoderick and R. H. Williams, *Metal-Semiconductor Contacts (Electrical & Electronic Engineering Monographs)*, 2nd ed. Oxford, U.K.: Oxford Univ. Press, 1988.
- [3] D. K. Schroeder, *Semiconductor Material and Device Characterization*, 3rd ed. New York: Wiley-Interscience, 2006.
- [4] F. Deng, R. A. Johnson, P. M. Asbeck, S. S. Lau, W. B. Dubbelday, T. Hsiao, and J. Woo, "Salicidation process using NiSi and its device application," *J. Appl. Phys.*, vol. 81, no. 12, pp. 8047–8051, Jun. 1997.
- [5] J. Liu and M. C. Ozturk, "Nickel germanosilicide contacts formed on heavily boron doped  $\text{Si}_{1-x}\text{Ge}_x$  source/drain junctions for nanoscale CMOS," *IEEE Trans. Electron Devices*, vol. 52, no. 7, pp. 1535–1540, Jul. 2005.
- [6] C. Fitz, M. Goldbach, A. Dupont, and S. Schmidbauer, "Silicides as contact material for DRAM applications," *Microelectron. Eng.*, vol. 82, no. 3/4, pp. 460–466, Dec. 2005.
- [7] O. Nakatsuka, K. Okubo, A. Sakai, M. Ogawa, Y. Yasuda, and S. Zaima, "Improvement in NiSi/Si contact properties with C-implantation," *Microelectron. Eng.*, vol. 82, no. 3/4, pp. 479–484, Dec. 2005.
- [8] D. B. Scott, R. A. Chapman, C. C. Wei, S. S. Mahantshetti, R. A. Haken, and T. C. Holloway, "Titanium disilicide contact resistivity and its impact on 1- $\mu\text{m}$  CMOS circuit performance," *IEEE Trans. Electron Devices*, vol. ED-34, no. 3, pp. 562–574, Mar. 1987.
- [9] S. M. Sze, *Physics of Semiconductor Devices*, 2nd ed. New York: Wiley-Interscience, 1981, pp. 304–307.
- [10] *The International Technology Roadmap for Semiconductors*, 2006. [Online]. Available: <http://www.itrs.net/Links/2006Update>
- [11] H. Iwai, T. Ohguro, and S. Ohmi, "NiSi salicide technology for scaled CMOS," *Microelectron. Eng.*, vol. 60, no. 1/2, pp. 157–169, Jan. 2002.
- [12] A. Lauwers, M. de Potter, O. Chamirion, R. Lindsay, C. Demeurisse, C. Vrancken, and K. Maex, "Silicides for the 100-nm node and beyond: Co-silicide, Co(Ni)-silicide and Ni-silicide," *Microelectron. Eng.*, vol. 64, no. 1–4, pp. 131–142, Oct. 2002.
- [13] A. Lauwers, J. A. Kittl, M. J. H. Van Dal, O. Chamirion, M. A. Pawlak, M. de Potter, R. Lindsay, T. Raynakers, X. Pages, B. Mebarki, T. Mandrekar, and K. Maex, "Ni based silicides for 45 nm CMOS and beyond," *Mater. Sci. Eng., B, Solid*, vol. 114/115, pp. 29–41, Dec. 2004.
- [14] M. C. Poon, M. Chan, W. Q. Zhang, F. Deng, and S. S. Lau, "Stability of NiSi in boron-doped polysilicon lines," *Microelectron. Reliab.*, vol. 38, no. 9, pp. 1499–1502, Sep. 1998.
- [15] D. Z. Chi, D. Mangelinck, A. S. Zuruzi, A. S. W. Wong, and S. K. Lahiri, "Nickel silicide as a contact material for submicron CMOS devices," *J. Electron. Mater.*, vol. 30, no. 12, pp. 1483–1488, Dec. 2001.
- [16] A. Lauwers, A. Steegen, M. de Potter, R. Lindsay, A. Satta, H. Bender, and K. Maex, "Materials aspects, electrical performance, and scalability of Ni silicide towards sub-0.13  $\mu\text{m}$  technologies," *J. Vac. Sci. Technol. B, Microelectron. Process. Phenom.*, vol. 19, no. 6, pp. 2026–2037, Nov./Dec. 2001.
- [17] S. S. Cohen, P. A. Piacente, G. Gildenblat, and D. M. Brown, "Platinum silicide ohmic contacts to shallow junctions in silicon," *J. Appl. Phys.*, vol. 53, no. 12, pp. 8856–8862, Dec. 1982.
- [18] S. Swirhun, K. C. Saraswat, and R. M. Swanson, "Contact resistance of LPCVD-W/Al and PtSi/W/Al metallization," *IEEE Electron Device Lett.*, vol. 5, no. 6, pp. 209–211, Jun. 1984.
- [19] H. C. W. Huang, R. Cook, D. R. Campbell, P. Ronsheim, W. Rausch, and B. Cunningham, "Platinum silicide contact to arsenic-doped polycrystalline silicon," *J. Appl. Phys.*, vol. 63, no. 4, pp. 1111–1116, Feb. 1988.
- [20] N. Stavitski, M. J. H. van Dal, R. A. M. Wolters, A. Y. Kovalgin, and J. Schmitz, "Specific contact resistance measurements of metal-semiconductor junctions," in *Proc. IEEE ICMTS*, Austin, TX, 2006, pp. 13–17.
- [21] R. L. Gillenwater, M. J. Hafich, and G. Y. Robinson, "Extraction of the minimum specific contact resistivity using Kelvin resistors," *IEEE Electron Device Lett.*, vol. EDL-7, no. 12, pp. 674–676, Dec. 1986.
- [22] A. S. Holland, G. K. Reeves, and P. W. Leech, "Universal error corrections for finite semiconductor resistivity in cross-Kelvin resistor test structures," *IEEE Trans. Electron Devices*, vol. 51, no. 6, pp. 914–919, Jun. 2004.